JTCM 中医杂志 Journal of Traditional Chinese Medicine

Online Submissions: http://www.journaltcm.com
info@journaltcm.com

J Tradit Chin Med 2016 February 15; 36(1): 107-112
ISSN 0255-2922

EXPERIMENTAL STUDY

Bloodletting at Jing-well points decreases interstitial fluid flow in the thalamus of rats

Fu Yu, Li Yuliang, GuoJia, Liu Bin, Liu Huipo, Zhang Weibo, Sun Wanli, Gao Yajuan, Ren Qiushi, Han Haojun

Fu Yu, Department of Neurology, Peking University Third Hospital, Beijing 100191, China
Ren Qiushi, Han Haojun, Beijing Key Lab of Magnetic Resonance Imaging Device and Technique, Beijing 100191, China; Department of Biomedical Engineering, College of engineering of Peking University, Beijing 100191, China
Li Yuliang, Liu Bin, Department of Interventional Medicine, The Second Hospital of Shandong University, Jinan 250033, China
Liu Huipo, Institute of Applied Physics and Computational Mathematics, Beijing 100094, China
Zhang Weibo, Institute of Acupuncture and Moxibustion China Academy of Chinese Medical Sciences, Beijing 100700, China
Guo Jia, Beijing Key Lab of Magnetic Resonance Imaging Device and Technique, Department of Biomedical Engineering, College of engineering of Peking University, Department of Radiology, Peking University Third Hospital, Beijing 100191, China
Sun Wanli, Gao Yajuan, Chang Zhi Medical College, Chang Zhi, 046000, China; Beijing Key Lab of Magnetic Resonance Imaging Device and Technique, Beijing 100191, China
Supported by the National Natural Science Foundation of China (Related Mechanisms and Basic Research of Citicolinein Treatment of Ultra-Early Cerebral Ischemia Delivery via Brain Interstitial, No. 81171080); the National Key Technology R&D Program for the 12th Five-year Plan (Advanced Cancer Treatment Equipment and Materials Development, No. 2012BAI15B009); National Key Developmental Program for Scientific Instruments and Equipment (Study of Delivery via Brain Interstitial Based on Multimodal Molecular Imaging Technology, No. 2011YQ030114); and a Seeding Grant for Medicine and Information Sciences of Peking University (Disciplinarian and Mechanism Research of Information Transmission and Interaction between Somatosensory Stimulation and Brain Tissue Channel, No. 2014-MI-12)
Correspondence to: Ren Qiushi, Han Haojun, Beijing Key Lab of Magnetic Resonance Imaging Device and Technique, Beijing 100191, China; Department of Biomedical Engineering, College of engineering of Peking University, Beijing 100191, China. renqsh@coe.pku.edu.cn; hhb1630@vip.sina.com

Telephone: +86-10-82266972
Accepted: September 23, 2015

Abstract

OBJECTIVE: To investigate the changes in the neuronal microenvironment of the middle cerebral artery (MCA) territory induced by Jing-well points bloodletting acupuncture (WPBA) and to explore the neuroprotective mechanism of WPBA in stroke.

METHODS: Adult male Sprague Dawley (n = 32) rats were randomly divided into four groups of eight animals each: WPBA-thalamus group (WT), WPBA-caudate nucleus group (WC), sham-control thalamus group (ST) and sham-control caudate nucleus group (SC). Animals in the WT and WC groups received 2 μL of the extracellular tracer gadolinium-diethylene triamine pentaacetic acid (Gd-DTPA) injected into the thalamus or caudate nucleus, respectively, and 12 Jing-well points in the distal ends of the rats' digits were used for WPBA. Although 2 μL of Gd-DTPA was injected into the thalamus or caudate nucleus, respectively, for animals in the two sham groups (ST and SC), no acupuncture or bloodletting was performed. Brain extracellular space and interstitial fluid flow parameters were measured using Gd-DTPA-enhanced magnetic resonance imaging.

RESULTS: The brain interstitial fluid flow speed was decreased in the thalamus after WPBA, with a significantly lower Gd-DTPA clearance rate and longer half-life of Gd-DTPA in the thalamus of treated rats than those in sham-control rats [WPBA-treated rats'

clearance rate, (7.47 ± 3.15) × 10^{-5}/s (P = 0.009); half-life, (1.52 ± 0.13) h, P = 0.000]. By contrast, no significant changes in brain extracellular space and interstitial fluid flow parameters were detected in the caudate nucleus after WPBA (P = 0.649). In addition, no differences in the morphology of the brain extracellular space or the final distribution of the traced brain interstitial fluid were demonstrated between the WT and WC groups (P = 0.631, P = 0.970, respectively).

CONCLUSION: The WPBA decreased the speed of the local thalamic ISF flow in rats, which is assumed to be a beneficial protection by down-modulated the metabolic rate of the attacked neurons under stroke.

Key words: Bloodletting; Extracellular space; Gadolinium ethoxybenzyl DTPA; Interstitial fluid; Magnetic resonance imaging

INTRODUCTION

Jing-well points bloodletting acupuncture (WPBA) is an ancient therapy in traditional Chinese medicine that has been used to treat stroke. The positive therapeutic effects observed following WPBA include a reduction in swelling and the removal of the obstruction in the meridian-collateral channels.[1,2] Recent evidence also indicates that WPBA effectively promotes blood circulation and modulates ion channel activity on neuronal membranes.[3-7] According to Traditional Chinese Medicine theory, meridians and collaterals compose a network of passages through which energy or *Qi* circulates and on which most acupuncture points are distributed.[8] Therefore, the network is equivalent neither to the vascular system nor to the nervous system. The extracellular space (ECS), surrounding neurons and capillaries in the brain tissue, has long been neglected in anatomical studies. However, by using a newly developed method based on magnetic resonance imaging (MRI), the interstitial fluid (ISF) flow can be dynamically visualized with the tracer gadolinium-diethylene triamine pentaacetic acid (Gd-DTPA) injected into the space.[9-12] In the present study, changes in the neuronal microenvironment were quantitatively measured after WPBA. Two sites commonly damaged during stroke were selected as the regions of interest, the thalamus and the caudate nucleus, which were supplied by the middle cerebral artery.[13] The neuroprotective mechanism of WPBA against cerebral stroke injury is discussed based on the findings.

METHODS

Animals

Thirty-two healthy, age-matched, adult male Sprague Dawley rats (250-300 g) of SPF grade were supplied by the laboratory animal center of Peking University Health Science Center (Certificate of quality No. SCXK [jing] 2011-0012). The experimental protocols were approved by the Ethics Committee of Peking University Health Center (No. LA2012-016).

Animal treatment and grouping

Thirty-two rats (n = 8 per group) were randomly divided into the following four groups by using a random number table: WPBA-thalamus group (WT), WPBA-caudate nucleus group (WC), sham-control thalamus group (ST), and sham-control caudate nucleus group (SC). Animals in the WT and WC groups received 2 μL of Gd-DTPA injected into the thalamus or caudate nucleus, respectively, and 12 Jing-well points in the distal ends of their digits were used for WPBA. Although 2 μL of Gd-DTPA was injected into the thalamus or caudate nucleus, respectively, for animals in the two sham groups (ST and SC), no acupuncture or bloodletting was performed.

Drugs and reagents

The Gd-DTPA solution was prepared using 10 mmol/L of Gd-DTPA (Magnevist; Bayer Schering Pharma AG, Berlin, Germany) diluted with 0.9% NaCl solution (Double-Crane Pharmaceutical Company Limited, China Resources, Beijing, China).

Intraparenchymal microinjection of Gd-DTPA into the brain

The skin overlying the calvaria of anesthetized rats was shaved and disinfected using iodinated alcohol. An incision was made on the scalp along the sagittal suture, from the midpoint of interaural line to the middle of the interocular line, and the skull was exposed by scraping away the skin and underlying tissues. The rats were placed in a stereotaxic instrument (Lab Standard Stereotaxic-Single, Stoelting Co., Wood Dale, Illinois, USA), and 2 μL of Gd-DTPA was administered by intracranial microinjection into the thalamus or caudate nucleus over 10 min. The stereotaxic coordinates for the thalamus were bregma − 2 mm, lateral − 2 mm, vertical − 5.5 mm, and those for the caudate nucleus were bregma+1 mm, lateral − 3 mm, and vertical − 4.5 mm. Rats were kept on a heating pad set at 38 ± 0.5 ℃ to maintain body temperature and the core temperature was monitored with a rectal thermometer.

Jing-well points bloodletting acupuncture

The 12 Jing-well points used for bloodletting were located in the distal ends of the digits and at the acupoints of Shaoshang (LU 11), Shangyang (LI 1), Zhongchong (PC 9), Guanchong (TE 1), Shaochong

(HT 9), and Shaoze (SI 1).[14] The bloodletting procedure was conducted by two physicians who applied pressure to restrict blood flow and to increase the visibility of veins. The vein was then swiftly pricked using a three-edged needle to a superficial depth of 2.5 mm, a few drops of blood were allowed to escape, and the point was pressed with sterile cotton until the bleeding stopped.

MRI scanning

Prior to MRI scans, all rats were anesthetized by intraperitoneal injection of a combined solution of pentobarbital sodium (26.58 mg/kg; Sigma, St. Louis, MO, USA), ethanol (427.5 mg/kg; Beijing Chemical Works, Beijing, China), chloral hydrate (127.5 mg/kg; Beijing Chemical Works, Beijing, China), magnesium sulfate (63.6 mg/kg; Beijing Chemical Works, Beijing, China), and propylene glycol (1.014 mL/kg; Beijing Chemical Works, Beijing, China). The anesthetic solution was administered every 2 hand the body temperature was maintained between 36.0 and 37.0 ℃ during the scanning process. A 3.0 T MRI system (Magnetom Trio, Siemens Medical Solutions, Erlangen, Germany) interfaced with an eight-channel wrist coil was used with a T1-weighted three-dimensional magnetization-prepared rapid acquisition gradient echo sequence. The rats underwent an MR pre-scan before tracer injection. Sequential MR scans were performed at 15, 30 min, 1, 2, 3, 4, 6, and 7 h after the tracer injection and bloodletting was completed in the WT and WC groups, and after the tracer injection in the ST and SC groups. The acquisition parameters were as follows: echo time, 3.7 ms; repetition time, 1500 ms; flip angle, 12°; inversion time, 900 ms; field of view, 267 mm; voxel, 0.5 × 0.5 × 0.5 mm^3; matrix, 512 × 512; number of averages, 2; phase encoding steps, 96. The acquisition time for each rat was 290 seconds.

MR image processing

Image post-processing was performed using a self-made software package based on Matlab (MathWorks, Natick, MA, USA). A mutual information-based method was used for deformable image registration.[15-17] The pre-scanned images were subtracted from post-scanned images. The signal attenuation (ΔSI) was automatically measured from the subtracted images and was converted to Gd-DTPA concentrations on a voxel-by-voxel basis.[16] The tracer diffusion coefficient and clearance rate were then derived from the concentration-time curve acquired from the sequential MR scans.

Calculations of the brain ECS and ISF flow parameters

ECS tortuosity was defined by $\lambda = (D/D^*)^{1/2}$, where D*and D represent the apparent diffusion coefficient and net diffusion coefficient in a given voxel, respectively. The ISF clearance rate was reflected by k'.[18] A standard method of least squares was used to extract D* and k', as described previously.[19,20] The acquisition of parameters was based on the assumption that cerebral ECS is a homogeneous porous medium in which molecular diffusion is isotropic with clearance following the first-order kinetic model. All voxels above a certain signal intensity threshold (two standard deviations [SD] above the brain background noise) were outlined to calculate the distribution volume ratio (Vd) of Gd-DTPA, which is a proportion of the Gd-DTPA distribution volume to the whole brain volume. The half-life of Gd-DTPA was calculated by the relationship $t_{1/2}$ = ln 2/clearance rate.

Statistical analysis

The experimental data were measured and calculated using Matlab software, without subjective factors. All numerical data are presented as the mean ± standard deviation ($\bar{x} \pm s$). Statistical analysis was performed using SPSS statistical software, version 13.0 (IBM SPSS Statistics for Windows, Armonk, New York, USA). One-way analysis of variance followed by individual comparisons of means was used for the comparison of different grouped data. Paired-samples *t* tests were used to compare two groups of data. *P* value less than 0.05 was considered to be significant.

RESULTS

Drainage and the final distribution of the Gd-DTPA tracer in the brain ISF after WPBA

WT versus ST: the accumulation of the Gd-DTPA-enhanced signal in the brain ISF was visualized as a hyper-signal intensity on MR images. The tracer was locally cleared, and no difference was found for the final maximal distribution of the traced ISF between the WT and ST groups. The enhancement was attenuated to normal in 2-3 h for the ST group, whereas the clearance took 6 h in WT group (Figure 1).

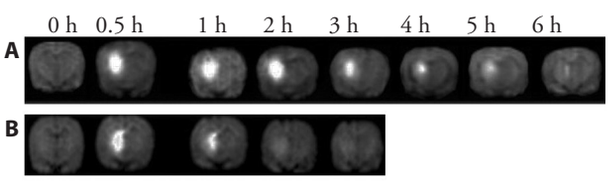

Figure 1 Representative coronal views of Gd-DTPA clearance in the thalamus of the rat brain

Enhanced MR signal intensity is represented as white. A: Gd-DTPA clearance in the Jing-WPBA-thalamus group (2 μL of Gd-DTPA injected into the thalamus and 12 Jing-Well points used in the distal ends of the digits for WPBA). B: Gd-DTPA clearance in the representative sham-control (ST group: 2 μL of Gd-DTPA injected into the thalamus, without WPBA). Gd-DTPA: gadolinium-diethylene triamine pentaacetic acid; WPBA: well points bloodletting acupuncture; MR: magnetic resonance imaging.

We found that k' in the WT group is significantly lower than that in the ST group, and that $t_{1/2}$ in the WT

group is significantly greater than that in the ST group. D* and λ are not significantly different between the two groups (Table 1).

WC versus SC: the Gd-DTPA tracer in the ISF primarily accumulated in the distal frontal and temporal cortices in both groups. No difference was found in the final maximal ISF distribution between the groups. The clearance of the Gd-DTPA tracer took 9-12 h in both groups, without a significant difference between the groups (paired *t*-test, P = 0.649; Figure 2). There are no significant differences between the two groups for D*, λ, k′, and $t_{1/2}$ (Table 2).

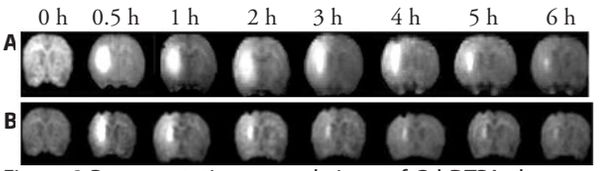

Figure 2 Representative coronal views of Gd-DTPA clearance in the caudate nucleus of the rat brain

The enhanced signal intensity on magnetic resonance image is represented as white. A: Gd-DTPA clearance in the Jing-WPBA-caudate nucleus (2 μL of Gd-DTPA injected into the caudate nucleus and 12 Jing-Well points in the distal ends of the digits used for WPBA). B: Gd-DTPA clearance in the respective sham-control caudate nucleus group (2 μLGd-DTPA injected into the caudate nucleus, without bloodletting). Gd-DTPA: gadolinium-diethylene triamine pentaacetic acid; WPBA: well points bloodletting acupuncture; MR:magnetic resonance imaging.

Drainage rate of brain ISF and tortuosity of brain ECS

The WPBA did not change the morphological structure (D*) of the ECS in the thalamus (P = 0.631) or caudate nucleus (P = 0.970) (paired *t*-tests, respectively).

However, the clearance rate of the Gd-DTPA tracer (k′) in the thalamus was significantly lower in the WT group than that in the ST group (paired *t*-test, P = 0.009; Table 1). Assuming that clearance follows a mono-exponential decay, the half-life in WT group was derived as 1.52 h, which was significantly greater than that of 0.81 h for the ST group (Table 1). For the caudate nucleus, the half-life of the Gd-DTPA tracer was (1.47 ± 0.24) h in the WC and (1.46 ± 0.56) h in the SC groups (paired *t*-test, P = 0.970; Table 2). No significant difference in clearance rate was found between the WC and SC groups (paired *t*-test, P = 0.649).

DISCUSSION

The present study demonstrated that WPBA effectively decreases the speed of the ISF flow in the thalamus, without altering local tortuosity.

The brain ISF is contained in a channel system surrounded by membranes of neural cells and capillaries. In the present study, we employed the *in vivo* tracer-based MRI method to detect the dynamic functional signal from the deep brain ISS, which is developed by Han HB and his colleagues. Due to the high resolution and feasibility to measure both the morphological and physiological parameters in the brain tissue channel, the method is so far the most optimal method to study the brain ISF flow and shows great potential for testing the merdian-collateral theory.[11] Theoretically, both neural cells and capillaries influence the ISF flow. However the vascular compartment occupies only 3%-5% of the brain volume,[9] and the Gd-DTPA tracer used in our study is an extracellular contrast agent with an extremely low permeability to the blood-brain barrier.[10,21] Therefore, it is reasonable to assume that the decreased brain ISF flow detected in our present study occurred mainly in the interstitial space rather the vascular compartment. By contrast, neural cells occupy 70%-80% of the brain volume. Thus, the cellular com-

Table 1 Structural and physiological parameters in the thalamus of the bloodletting and control groups ($\bar{x} \pm s$)

Group	D* ($\times 10^{-4}$mm^2/s)	λ	k' ($\times 10^{-5}$/s)	$t_{1/2}$ (h)
WT	3.36±0.93	1.29±0.32	7.47±3.15	1.52±0.13
ST	3.28±0.67	1.28±0.17	14.40±4.50	0.81±0.03
P value	0.631	0.631	0.009	0.000

Notes: WT: Jing-well points bloodletting acupuncture-thalamus group (2 μL Gd-DTPA injected into the thalamus and 12 Jing-well points in the distal ends of the digits used for WPBA); ST: sham-control thalamus group (2 μL Gd-DTPA injected into the thalamus, without bloodletting); Gd-DTPA: gadolinium-diethylene triamine pentaacetic acid; WPBA: well points bloodletting acupuncture; D*: effective diffusion coefficient; λ: tortuosity; k′; clearance rate of the tracer; $t_{1/2}$: half-life; *P* value: comparison of WT and ST groups.

Table 2 Brain structural and physiological parameters in the caudate nucleus of the bloodletting and control groups ($\bar{x} \pm s$)

Group	D* ($\times 10^4$ mm^2/s)	λ	k' ($\times 10^{-5}$/s)	$t_{1/2}$ (h)
WC	3.37±0.93	1.31±0.52	7.90±2.10	1.47±0.24
SC	3.38±1.08	1.31±0.31	7.84±4.18	1.46±0.56
P value	0.970	0.970	0.649	0.673

Notes: WC: Jing-WPBA-caudate nucleus group (2μL of Gd-DTPA injected into the caudate nucleus and 12 Jing-well points in the distal ends of the digits used for WPBA; SC: sham-control caudate nucleus group (2μL of Gd-DTPA injected into the caudate nucleus, without bloodletting); Gd-DTPA: gadolinium-diethylene triamine pentaacetic acid; WPBA: well points bloodletting acupuncture; D*: effective diffusion coefficient; λ: tortuosity; k′: clearance rate of the tracer; $t_{1/2}$: half-life; *P* value: comparison of WC and SC groups.

partment is likely to contribute more to the decrease in brain ISF flow. Because neuronal nutrients and the metabolic waste are transported *via* the brain ISF, its flow rate should be strongly correlated with the metabolic rate of the neurons or their excitatory state. According to our previous results, the ISF drainage rate in the thalamus was faster than that in the caudate nucleus or olfactory bulbs,[19] consistent with previous results demonstrated using 18F-fluorodeoxyglucose.[22] A lower metabolic rate induced by either anti-excitation or injection of anesthetic drugs provides beneficial protection for ischemic neurons,[23] a finding that also supports the assumption that the slowdown in the ISF drainage rate was caused by a regional down-modulation of the metabolic rate, which potentially offers neuroprotection during an ischemic or hemorrhagic attack.

The biophysical property of the brain interstitial space is the other key factor for understanding the ISF flow speed. According to the results in present study, the tortuosity of the ECS was not changed with WPBA, indicating that the slowdown in the ISF flow was not caused by local tortuosity but by decreased secretion or changes in the brain ISF drainage route.[24] Most previous studies have demonstrated that the ISF clears the brain by following the lymphatic drainage of the head and neck, and a close connection between brain ISF and cerebrospinal fluid (CSF) cycles has been proposed.[19,25,26]

Our previous study has verified that the ISF from the brain deep center caudate nucleus drains into the CSF compartment around the olfactory bulbs,[19] which will finally drain to the cervical lymph nodes via the nasal lymphatics.[27,28] The results of all these aforementioned studies suggest a potential connection between central brain ISF flow and peripheral tissue interstitial channels.

The Jing-well point bloodletting therapy is not a simple treatment. It can lead to at least four biological results: bleeding, point acupuncture, pain stimulation, and the release of local interstitial fluid. Most previous analyses examining the mechanism of acupuncture therapy effects on stroke were focused on bleeding. However, during bloodletting therapy, blood and interstitial fluid are simultaneously released. Originally, stroke was thought to be caused by a vicious wind that penetrated the brain center and disrupted brain function, with the wind's turbulence generating heat and phlegm stagnation in blood. The heat was thought to be discharged by the blood released at Jing-well points because blood was considered a vehicle for removing excess heat.[14] However, it is currently known that the peripheral blood is the same blood that circulates throughout the entire body; thus, there is no reason to expect that bleeding removes excess heat. In addition to blood, bloodletting acupuncture releases a small amount of ISF in the extremities. Because the lymphatic route is an ISF drainage passage, the correlation between the lymphatic system and the bloodletting Jing-well points needs further investigation.

In conclusion, the effect of WPBA to reduce the brain ISF flow rate in the thalamus provides a new perspective in understanding the mechanism of Jing-well points bloodletting acupuncture therapy in stroke.

ACKNOWLEDGMENT

We would like to express sincere gratitude to Han Hongbin, a professor of Radiology in Peking University Third Hospital and the Director of Beijing Key Lab of Magnetic Resonance Imaging Device and Technique, for his technical guidance and instructive advice in the design and execution of this study.

REFERENCES

1 **Duan GB**. Clinical application of twelve well points in emergency treatment. World J Acup Max 2000; 10(2): 48-50.

2 **Guo Y**, Wang XY, Xu TP, Dai ZH, Li YC. Clinical observation of the influence of puncture and blood letting at twelve Hand Well-Jing Point on consciousness and heart rate in patients with wind-stroke. Tianjin Zhong Yi Yao 2003; 20(2): 35-37.

3 **Guo Y**, Zhang YJ, Wang XY, et al. Effects of blood-letting puncture at hand twelve Well-Jing(well)-points on intracranial hemodynamics of stroke patients. Zhen Jiu Lin Chuang Za Zhi 1995; 11(6): 21-23.

4 **Ma YF**, Guo Y, Zhang YJ, Xu TP, Bao JZ. Dynamic observation of the influence of blood-letting puncture of hand twelve well points on partial pressure of oxygen in ischemic brain tissue in rats with experimental cerebral ischemia. Shanghai Zhen Jiu Za Zhi 2000; 19(1): 40-42.

5 **He SQ**, Guo Y, Ma YF, Miao WF, Wang XY. Experimental study about the influence of blood-letting puncture at hand twelve Well-Jing (well)-points on H^+ concentration of ischemic brain tissue in rats with experimental cerebral ischemia. Zhen Jiu Lin Chuang Za Zhi 2002; 18(2): 43-44.

6 **Liu HL**, Zhang DS, Tan XG, et al. The effect of acupuncture on stroke recovery: study protocol for a randomized controlled trial. BMC Complement Altern Med 2012; 12: 216

7 **Lu X**, Chen ZL, Guo Y, et al. Blood-letting punctures at twelve Jing-well points of the hand can treat cerebral ischemia in a similar manner to mannitol. Neural Regen Res 2013; 8(6): 532-539.

8 **Ni MS (translator)**. The Yellow Emperor's Classic of Medicine. Boston: Shambhala Publishing House, 1995: 17-26.

9 **Shi C**, Lei Y, Han H, et al. Transportation in the interstitial space of the brain can be regulated by neuronal excitation. Sci Rep 2015; 5: 17673.

10 **Caravan P**, Ellison JJ, McMurry TJ, Lauffer RB. Gadolinium (Ⅲ) Chelates as MRI contrast agents: structure, dynamics, and applications. Chem Rev 1999; 99(9): 2293-2352.

11 **Han HB**. The calculated morphological and physiological parameters of brain ISF and ECS. China Patent: 200980126605.2. 2009 Aug 1.

12 **Han HB**, Xia ZL, Chen H, Hou C, Li WB. Simple diffusion delivery *via* brain interstitial route for the treatment of cerebral ischemia. Sci China Life Sci 2011; 54(3): 235-239.

13 **Bogousslavsky J**, Barnett HJ, Fox AJ, Hachinski VC, Taylor W. Atherosclerotic disease of the middle cerebral artery. Stroke 1986; 17(6): 1112-1120.

14 **Ahn AC**, Schnyer R, Conboy L, Laufer MR, Wayne PM. Wayne Electrodermal Measures of Jing-Well Points and Their Clinical Relevance in Endometriosis-Related Chronic Pelvic Pain. J Altern Complement Med 2009; 15(12): 1293-1305.

15 **Viola P**, Wells III WM. Alignment by maximization of mutual information. Int J Comput Vision 1997; 24(2): 137-154.

16 **Studholme C**, Drapaca C, Iordanova B, Cardenas V. Deformation-based mapping of volume change from serial brain MRI in the presence of local tissue contrast change. IEEE Trans Med Imaging 2006; 25(5): 626-639.

17 **Han H**, Shi C, Fu Y, et al. A novel MRI tracer-based method for measuring water diffusion in the extracellular space of the rat brain. IEEE J Biomed Health Inform 2014; 18(3): 978-983.

18 **Xu F**, Han H, Zhang H, Pi J, Fu Y. Quantification of Gd-DTPA concentration in neuroimaging using T1 3D MP-RAGE sequence at 3.0 T. Magn Reson Imaging 2011; 29(6): 827-834.

19 **Han H**, Li K, Yan J, Zhu K, Fu Y. An *in vivo* study with an MRI tracer method reveals the biophysical properties of interstitial fluid in the rat brain. Sci China Life Sci 2012; 55(9): 782-787.

20 **Li K**, Han H, Zhu K, et al. Real-time magnetic resonance imaging visualization and quantitative assessment of diffusion in the cerebral extracellular space of C6 glioma-bearing rats. Neurosci Lett 2013; 543: 84-89.

21 **Larsson HB**, Tofts PS. Measurement of blood-brain barrier permeability using dynamic Gd-DTPA scanning--a comparison of methods. Magn Reson Med 1992; 24(1): 174-176.

22 **Abbott NJ**. Evidence for bulk flow of brain interstitial fluid: significance for physiology and pathology. NeurochemInt 2004; 45(4): 545-552.

23 **Heiss WD**, Habedank B, Klein JC, et al. Metabolic rates in small brain nuclei determined by high-resolution PET. J Nucl Med 2004; 45(11): 1811-1815.

24 **Sloop CH**, Dory L, Roheim PS. Interstitial fluid lipoproteins. J Lip Res 1987; 28(3): 225-237.

25 **Cserr HF**, Cooper DN, Milhorat TH. Flow of cerebral interstitial fluid as indicated by the removal of extracellular markers from rat caudate nucleus. Exp Eye Res 1977; 25 Suppl: 461-473.

26 **Carare RO**, Bernardes-Silva M, Newman TA, et al. Solutes, but not cells, drain from the brain parenchyma along basement membranes of capillaries and arteries: significance for cerebral amyloid angiopathy and neuroimmunology. Neuropathol Appl Neurobio 2008; 34(2): 131-144.

27 **Muldoon LL**, Varallyay P, Kraemer DF, et al. Trafficking of superparamagnetic iron oxide particles (combidex) from brain to lymph nodes in the rat. Neuropathol Appl Neurobio 2004; 30(1): 70-79.

28 **Weller RO**, Galea I, Carare RO, Minagar A. Pathophysiology of the lymphatic drainage of the central nervous system: implications for pathogenesis and therapy of multiple sclerosis. Pathophysiology 2010; 17(4): 295-306.